



Bennettitalean Leaves From the Permian of Equatorial Pangea—The Early Radiation of an Iconic Mesozoic Gymnosperm Group

Patrick Blomenkemper^{1*}, Robert Bäumer¹, Malte Backer¹, Abdalla Abu Hamad², Jun Wang^{3,4}, Hans Kerp¹ and Benjamin Bomfleur^{1*}

¹ Palaeobotany Research Group, Institute of Geology and Palaeontology, Westfälische Wilhelms-Universität Münster, Münster, Germany, ² Environmental and Applied Geology Department, The University of Jordan, Amman, Jordan, ³ State Key Laboratory of Palaeobiology and Stratigraphy, Nanjing Institute of Geology and Palaeontology and Center for Excellence in Life and Palaeoenvironment, Chinese Academy of Sciences, Nanjing, China, ⁴ College of Earth and Planetary Sciences, University of Chinese Academy of Sciences, Beijing, China

OPEN ACCESS

Edited by:

Evelyn Kustatscher,
Museum of Nature South Tyrol, Italy

Reviewed by:

William DiMichele,
Smithsonian Institution, United States
Mihai Emilian Popa,
University of Bucharest, Romania

*Correspondence:

Patrick Blomenkemper
p_blom02@uni-muenster.de
Benjamin Bomfleur
bbomfleur@uni-muenster.de

Specialty section:

This article was submitted to
Paleontology,
a section of the journal
Frontiers in Earth Science

Received: 12 January 2021

Accepted: 24 February 2021

Published: 26 March 2021

Citation:

Blomenkemper P, Bäumer R,
Backer M, Abu Hamad A, Wang J,
Kerp H and Bomfleur B (2021)
Bennettitalean Leaves From
the Permian of Equatorial
Pangea—The Early Radiation of an
Iconic Mesozoic Gymnosperm Group.
Front. Earth Sci. 9:652699.
doi: 10.3389/feart.2021.652699

Bennettitaleans are an extinct group of gymnosperms that are among the most iconic plants of Earth's vegetation during the Mesozoic Era. The sudden appearance and rise to dominance of the Bennettitales during the Triassic remains a mystery. Leaf fossils similar to typical bennettitalean foliage occur in late Paleozoic deposits worldwide, but bennettitalean foliage can be identified with certainty only in case the fossils are sufficiently well-preserved to show epidermal features. So far, the characteristic stomatal architecture of the group has never been systematically documented in these putative Paleozoic remains. Here, we present well-preserved bennettitalean leaves from Permian deposits in two widely separated regions of equatorial Pangea. Two species of cuticle-bearing leaf compressions from the late Permian Umm Irna Formation, Jordan, are here formally described as *Pterophyllum pottii* Bomfleur et Kerp sp. nov. and *Nilssoniopteris jogiana* Blomenkemper et Abu Hamad sp. nov. Moreover, bulk maceration of samples from the Umm Irna Formation yielded six additional types of dispersed bennettitalean cuticles that are here informally described. In addition, the Cisuralian (early Permian) uppermost part of the Upper Shihhotse Formation exposed at the Palougou section in Shanxi Province, China, has yielded the oldest unambiguous bennettitalean fossils known to date; they consist of fragments of entire-margined leaves with well-preserved cuticles that we assign to *Nilssoniopteris shanxiensis* Bäumer, Backer et Wang sp. nov. Unlike the characteristic puzzle-patterned cuticles typical of many Jurassic and Cretaceous bennettitales, the cuticles of these Permian bennettitalean remains show non-sinuuous anticlinal walls, greater variety in stomatal orientation, and rare occurrence of transversely divided subsidiary cells—features that have until now almost exclusively been documented from the hitherto oldest cuticle-bearing Triassic

bennettitalean material. Finally, the taxonomic richness, disjunct distribution, and broad variety in macro- and micromorphological features in these Permian bennettitalean remains lead us to suspect that the origin of the group will date back still further in time, and might in fact coincide with very early occurrences of Bennettitales-like foliage from the Pennsylvanian and Cisuralian, such as *Pterophyllum cottaeanum*, *P. eratum*, or *P. grandeuryi*.

Keywords: Bennettitales, Cycadeoidales, cuticle analysis, Lopingian, Pangea

INTRODUCTION

The end-Permian biotic crisis is the largest of the five Phanerozoic mass extinctions (e.g., Erwin, 1993) and the oldest that also affected terrestrial biotas. Detailed assessment of the degree and abruptness of species turnover during this critical time interval, however, requires robust knowledge of the pre-extinction diversity and community composition. This poses several problems considering the plant-fossil record in particular. Late Permian macrofloras are rare (Bernardi et al., 2017) and most records spanning the P-T boundary are based on microfloras from marine deposits (e.g., Hochuli et al., 2010; Nowak et al., 2019). The Permian, particularly the late Permian, is marked by a very distinct floral provincialism, which is now commonly regarded as an expression of a climate-related global floral zonation, making direct comparisons between different provinces extremely difficult. Moreover, at least in Europe, most floras are allochthonous and we have no idea what the actual vegetation looked like; pteridophytes, for instance, are extremely rare in macrofloral associations that are dominated by xerophilous elements, but their presence, even though as minor constituents, is evidenced by the palynological record (e.g., Grebe, 1956; Grebe and Schweitzer, 1962; Schneebeli-Hermann et al., 2015, 2017). By contrast, in China hygrophilous elements usually prevail (Ouyang and Utting, 1990; Peng et al., 2006; Yin et al., 2007).

Over the last 20 years a series of localities in the late Permian Umm Irna Formation of Jordan has yielded very rich and diverse macrofloral associations, varying from ones from humid settings with calamitaleans and pectopterids to others with taxa adapted to drier conditions, like conifers. Most remarkable is that taxa considered to be typical for different floral provinces are found in the different facies of the same formation, and—in some localities—even within the same bed. Taken together, the flora comprises taxa typical for Cathaysia, Gondwana, and Euramerica. Moreover, some taxa appear to have persisted much longer than originally thought, such as the walchian conifer *Otovicia hypnoides*, a very long-ranging species that has its last appearance in the upper Permian of Jordan. The first occurrences of at least three major lineages of gymnospermous plants that were traditionally regarded as typically Mesozoic were reported from the upper Permian of Jordan (Kerp et al., 2006; Abu Hamad et al., 2008, 2017; Blomenkemper et al., 2018, 2020). Most common are corystosperms of which first foliage assignable to *Dicroidium* was described (Kerp et al., 2006; Abu Hamad et al., 2008, 2017), and recently also fertile organs (Blomenkemper et al., 2020). *Dicroidium* is a genus that is traditionally regarded

as a marker for the Triassic of Gondwana (Anderson et al., 1996). In addition, Blomenkemper et al. (2018) briefly reported two other groups of plants from the Umm Irna Formation that appear much earlier than previously thought, i.e., podocarpacean conifers and bennettitaleans.

Bennettitales are a peculiar group of extinct gymnosperms with a growth habit and foliage closely resembling that of cycads. However, the reproductive organs are very different. Cycadaleans have either simple megasporophylls with ovules attached to the lower part and a distal foliar blade in the Cycadaceae, or ovule-bearing woody cones in the Zamiaceae. The pollen organs consist of small cones. All modern cycadaleans are dioecious. By contrast, bennettitaleans had very complex flower-like reproductive organs; some were bisexual, whereas others had separate ovule-bearing and pollen organs, but it is not known whether these were borne on the same plant. Unfortunately, foliage—by far the most common fossil of the Bennettitales—resembles that of the Cycadales so closely that tracking their evolutionary history through space and time is only viable when epidermal details are preserved. Whereas cycads have haplocheilic stomata consisting of two guard cells surrounded by a ring of subsidiary cells like in most pteridosperms and conifers, the syndetocheilic stomata of the bennettitaleans and the guard and subsidiary cells all developed from a single initial cell, giving the stomatal apparatus a completely different appearance (Thomas and Bancroft, 1913; Florin, 1933). The oldest bennettitaleans were reported from the Middle Triassic (Wachtler and Van Konijnenburg-van Cittert, 2000; Kustatscher and Van Konijnenburg-van Cittert, 2005; McLoughlin et al., 2018) but these records are all based on macromorphological characters only. Although Cycadales and Bennettitales are usually classified within the Cycadophytes, their relationship is still unclear and little is known about the early history of these two groups.

In addition to two new species from the late Permian Umm Irna Formation of Jordan, we here describe a third new, even older species of entire-margined bennettitalean leaf from the lower Permian of Shanxi, China. All three species are based on macrofossils with preserved epidermal details. Apart from these, bulk macerations of sediments of the Umm Irna Formation revealed several types of dispersed cuticles showing typical bennettitalean stomata. The here described finds from China and Jordan are the oldest *bona fide* records of the Bennettitales known so far. They show that this group of “typical Mesozoic” gymnosperms was already well-diversified and widespread during the latest Paleozoic.

MATERIALS AND METHODS

The studied material consists of cuticle-bearing compression fossils and dispersed cuticles of bennettitalean leaves from the Changhsingian (latest Permian; see Powell et al., 2016, 2019). Umm Irna Formation, Dead Sea region, Jordan, and from the Cisuralian (early Permian; see Wu et al., 2021) upper part of the Upper Shihhotse Formation, Shanxi Province, China.

The Umm Irna Formation is an up to 85 m-thick succession of Permian alluvial deposits exposed along the northeastern shore of the Dead Sea, Jordan. It overlies the Cambrian Umm Ishrin Sandstone Formation and is itself overlain by the basal Triassic Ma'in Formation (Powell et al., 2016, 2019). Sediments of the Umm Irna Formation were deposited in a fluviolacustrine lowland setting under strongly seasonal conditions (e.g., Bandel and Khoury, 1981; Stephenson and Powell, 2013). The formation has yielded a peculiar admixture of plant taxa, including typical late Paleozoic and Mesozoic taxa as well as typical representatives from different floral provinces of Pangea (Mustafa, 2003; Kerp et al., 2006; Abu Hamad et al., 2008, 2017; Blomenkemper et al., 2018, 2019, 2020; Zavialova et al., 2021). Bennettitalean fossils have been recovered from three fossil localities in particular: (1) site "JO5," a N-S-trending cliff outcrop informally referred to as "Dyke Plateau main locality" (N31°32'3", E35°33'27"; locality 7 of Stephenson and Powell, 2013), ~15 km south of the mouth of Wadi Zarqa Ma'in along eastern shore of the Dead Sea; (2) site "JO4," a roadcut outcrop immediately opposite to the entrance road to the "Dyke Plateau"; and (3) site "JO5a," a natural exposure along the southern flank of a small E-W-trending gully at the northern part of the "Dyke Plateau" (31°32'7"N, 35°33'31"E; locality 123 of Abu Hamad et al., 2016), about 200 m west of Highway 65 and approximately 100 m northeast of the central Dyke Plateau outcrop.

Material from the Upper Shihhotse Formation was collected in 2018 from one particular bed (bed 137 of Liu et al., 2015) near the top of the formation exposed in the Palougou section along Xiaohegou River, Shanxi Province, China, where the upper part of the Upper Shihhotse Formation consists of an alternating succession of barren red beds with intercalations of reddish-brown, locally fossil-rich mudstone and thick, lenticular stacks of coarse-grained sandstones (Liu et al., 2015).

Chemical Preparation

Bulk macerated material and *in situ* samples were treated following standard methods detailed in Kerp (1990) and Krings and Kerp (1997) using hydrofluoric acid (HF 40%) to dissolve the rock matrix or remove remaining sediment particles from *in situ* samples. Cuticles were treated afterward with Schulze's reagent [nitric acid (15–30% HNO₃) and a little potassium chlorate (KClO₃)], neutralized, treated with potassium hydroxide (4% KOH) and rinsed in distilled water. If necessary, specimens still too dark for light microscopy analysis were carefully treated with standard household bleach (4% sodium hypochlorite solution NaHClO₂).

Photography

Hand specimens were photographed using a Canon EOS 5D Mark VI digital camera following the methods detailed in Kerp and Bomfleur (2011). Cuticle specimens were photographed using a Leica DM5500B microscope equipped with epifluorescence and a Leica DFC450 digital camera head. If necessary, small adjustments, e.g., in brightness and contrast, were carried out in standard imaging software (Adobe Photoshop CC; Affinity Photo).

SYSTEMATIC PALEONTOLOGY

Gymnospermatophyta

Order Bennettitales Engler, 1892

Family incertae sedis

Genus *Pterophyllum* Brongniart, 1825 *nom. cons.*

Type Species

Pterophyllum filicoides (Schlotheim, 1822) Zeiller, 1906 *typ. cons.*

Pterophyllum pottii Bomfleur et Kerp *sp. nov.*

Figures 1A–K

Diagnosis

Leaves evenly divided into large, laterally inserted, parallel-margined and parallel-veined segments with expanded bases. Leaves amphistomatic with well-defined costal and intercostal fields; stomatal density lower on upper surfaces. Stomata syndetocheilic; in rare cases subsidiary cells transversely divided. Stomatal pores predominantly transversely aligned, with a distinct ledge covering each pole. Epidermal cells with distinct, longitudinal striae; anticlinal walls overall straight but in many cases minutely sinuous.

Holotype (Hic Designatus)

Cuticle-bearing compression fossil of a leaf fragment (JO15-5-115) with a cuticle fragment mounted on permanent slide JO15-5-115-SL#001 for transmitted-light microscopy.

Additional Material

Four cuticle-bearing compression fossils (JO17-4B-92, JO17-4B-94, JO15-4-33, JO15-4-24) and 25 permanent slides with mounted cuticle fragments extracted either *in situ* or via bulk maceration of selected hand samples (JO15-5-115#SL001; BULK_JO15-4-43SL#001–002, 004–005, 007–010; BULK_JO17-4B-47SL#001–008; JO17-4B-SL#001–005; BULK_JO15-4-43SL#003, 006; BULK_JO15-4-53SL#004).

Type Locality

Natural exposure of the Umm Irna Formation informally referred to as "Dyke Plateau" (N31°32'3", E35°33'27"; locality 7 of Stephenson and Powell, 2013), ~15 km south of the mouth of Wadi Zarqa Ma'in, along eastern shore of the Dead Sea, Jordan.

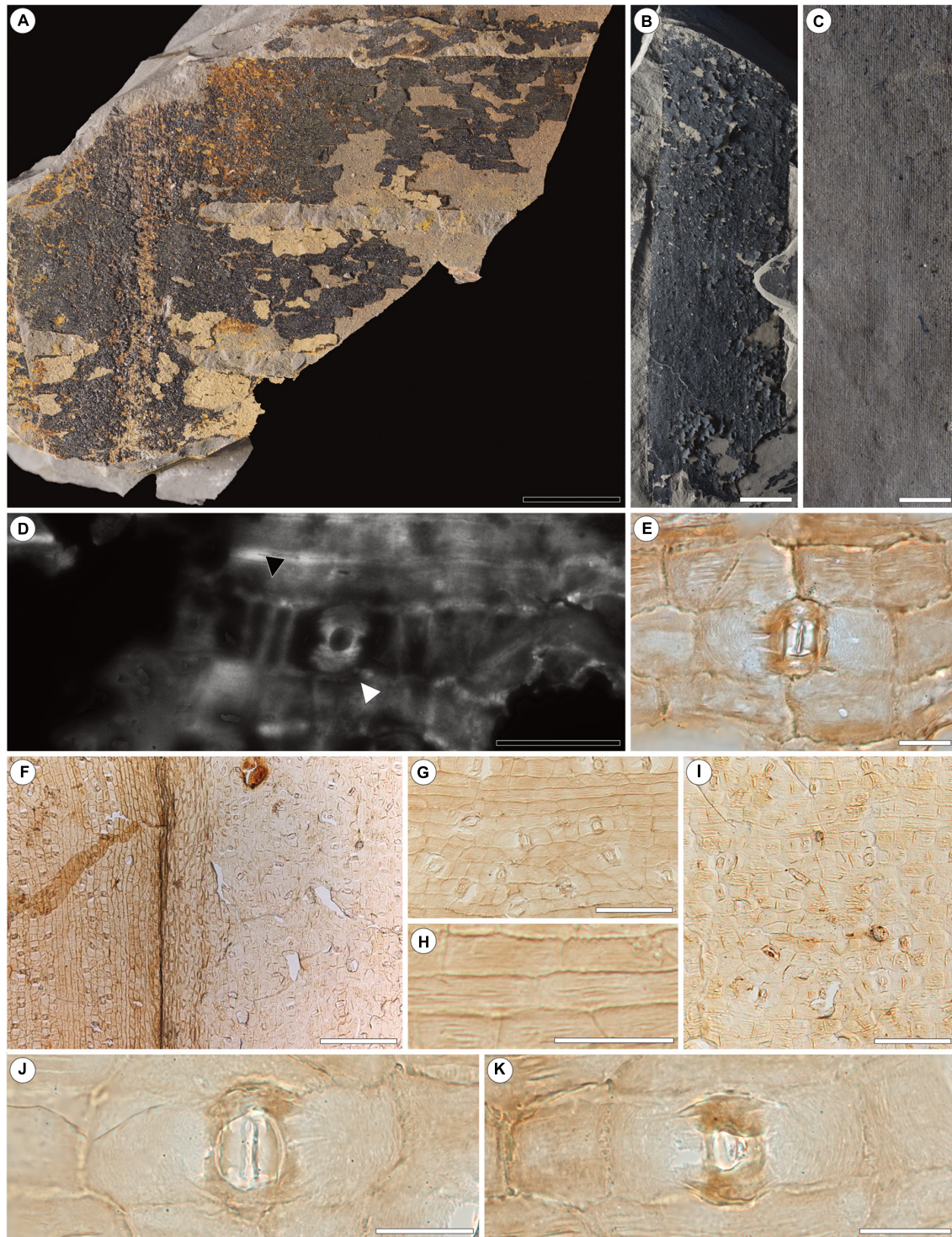


FIGURE 1 | *Pterophyllum pottii* Bomfleur et Kerp sp. nov. from the upper Permian of Jordan (A–K). (A) Designated holotype of *P. pottii* (JO15-5-115) showing the leaf morphology. (B,C) Isolated leaf fragment of *P. pottii*. (B) Leaf fragment with well-preserved cuticles loosely adhering to the matrix. (C) Counterpart of (B) showing the dense parallel venation. (D) Epifluorescence picture of a typical stoma of the holotype. Note the typical striate ledge of *P. pottii* (white arrow), palisade like subdivision (black arrow) and fragmentary preservation of the cuticle compared to (E–J). (E) Typical stoma in transmitted light from (B). (F) Lower (right) and upper (left) surface of *P. pottii*. Note the difference in stomatal density. (G) Upper leaf surface of *P. pottii*. (H) Detail of (G) showing the distinct striation on the periclinal walls. (H) Detail of (G) showing the longitudinal striae on periclinal walls and slightly undulating anticlinal walls. (I) Lower leaf surface of *P. pottii*. Note the difference in epidermal cell sizes. (J,K) Enlarged stomata of the lower leaf surface. Note the strongly thickened, overhanging polar ledges. Scale bars for (A,B) = 1 cm; (C) = 5 mm; (D) = 50 μm ; (E) = 20 μm ; (F) 200 μm ; (G) = 100 μm ; (H) = 50 μm ; (I) = 100 μm ; (J,K) = 20 μm .

Type Stratum and Age

Umm Irna Formation; Changhsingian (late Lopingian, late Permian).

Etymology

The specific epithet is chosen in honor of our friend and colleague Christian Pott (Münster, Germany) for his substantial contributions to our knowledge of the Bennettiales.

Description

The holotype (JO15-5-115) is a 5 cm long and 6 cm wide leaf fragment (**Figure 1A**) with preserved epidermal details. Rachis 5–6 mm wide with laterally inserted segments. Individual segments about 15–20 mm wide. Venation dense, veins running parallel to the segment margin; about 42–48 veins per transversal 10 mm. Additional specimens (**Figures 1B,C**) up to 11 cm long and 3 cm wide. Apices of individual segments not preserved. Leaf is amphistomatic, thin. Cuticles of upper and lower leaf surfaces with distinctive costal and intercostal fields (**Figures 1F–H**). Additional specimens (**Figures 1B,C**) demonstrate that individual segments reach up to 40 mm in width.

Cuticles of upper leaf surfaces thinner. Intercostal fields up to 130 μm wide; costal fields up to about 80 μm wide. Stomatal complexes syndetocheilic, confined to intercostal fields; closely spaced on lower leaf surfaces (**Figures 1F,G**), loosely spaced on upper leaf surfaces (**Figures 1E,I**). Most stomatal complexes with two, some with up to four subsidiary cells (**Figures 1D,E,J,K**); anti- and periclinal walls smooth. Stomatal pores predominantly transversely oriented, occasionally oriented obliquely or perpendicular; both poles of stomatal pores commonly covered by a striated ledge (**Figures 1D,E,J,K**). Ordinary epidermal cells of costal fields rectangular, elongate, up to twice as long as wide; anticlinal walls slightly undulating (**Figure 1H**). Epidermal cells of the intercostal fields (**Figures 1G,H**) predominantly isodiametric rectangular. All periclinal walls of ordinary epidermal cells with distinct, longitudinal striae (**Figure 1H**). Trichome bases are absent.

Comparisons and Remarks

Co-occurring cycadalean leaves with superficially similar architecture (e.g., *Pseudoctenis*) are readily distinguished by their haplocheilic stomata. Compared to other species of *Pterophyllum* with known epidermal details, *P. pottii* is delimited by its amphistomatic leaf (Harris, 1969; Pott et al., 2007c, 2016). *Pterophyllum pottii* differs from *P. fontarium* (Watson and Sincock, 1992) in having distinct ledges covering the poles of the stomatal pore, in having longitudinal striae on the epidermal cells, and in showing only finely sinuous anticlinal walls.

The most prominent feature of *Pterophyllum pottii* is the well-developed striation of the ordinary epidermal cells (**Figure 1H**) and some of the polar thickenings of the stomatal complexes (**Figures 1D,E,J,K**). Similar structures have been reported previously, e.g., from *Glossophyllum florinii*, a putative ginkgophyte from the Upper Triassic (Pott et al., 2007a).

Genus *Nilssoniopteris* Nathorst, 1909, emend. Pott et al., 2007b

Type Species

Nilssoniopteris solitaria (Phillips, 1829) Cleal and Rees, 2003

Nilssoniopteris jogiana Blomenkemper et Abu Hamad sp. nov.

Figures 2A–G

Diagnosis

Leaf simple, elongate, entire-margined; rachis straight, with longitudinally striations; lamina laterally attached to rachis. Leaf imperfectly amphistomatic with most stomata on lower surface; lower lamina with distinct costal and intercostal fields. Stomatal complexes syndetocheilic, confined to intercostal fields, evenly spaced, with transversely oriented pores. Anticlinal walls of subsidiary and epidermal cells smooth, straight to slightly curved.

Holotype (Hic Designatus)

Cuticle-bearing compression fossil of a leaf fragment (JO15-5-62), with cuticle fragments mounted on four permanent slides (JO15-5-62SL#001–004) for transmitted-light microscopy.

Type Locality

Natural exposure of the Umm Irna Formation informally referred to as “Dyke Plateau” (N31°32'3", E35°33'27"; locality 7 of Stephenson and Powell, 2013), ~15 km south of the mouth of Wadi Zarqa Ma'in, along eastern shore of the Dead Sea, Jordan.

Type Stratum and Age

Umm Irna Formation; Changhsingian (late Lopingian, late Permian).

Etymology

The specific epithet is chosen in honor of our friend and colleague Jörg “Jogi” Schneider (Freiberg, Germany) for his manifold contributions to our knowledge of late Paleozoic fossils and biostratigraphy.

Description

The holotype (**Figures 2A–H**) is a partially preserved, relatively large leaf fragment, about 17 cm long and 5 cm wide; leaf lamina attached laterally at the longitudinally striate rachis (**Figure 2B**). Width of the rachis close to the presumed basal portion about 3 mm, increasing to about 4–5 mm at the apical portion; widest preserved lamina portion is 3 cm in width close to the presumed leaf base. Marginal areas of the leaf lamina not preserved.

The leaf is imperfectly amphistomatic. Lower leaf surfaces are divided into distinct costal and intercostal fields (**Figures 2C,D**); stomata on the lower leaf surfaces are evenly spaced, confined to the intercostal fields. Stomatal complexes syndetocheilic with two lateral subsidiary cells (**Figures 2C,E–H**); nearly all stomatal pores transversely aligned, rarely deviating at slight angles (**Figure 2C**). Guard cells more strongly cutinized than surrounding epidermal and subsidiary cells (**Figure 2H**). Anticlinal and periclinal walls of the subsidiary cells smooth. Ordinary epidermal cells in intercostal fields of the lower surface

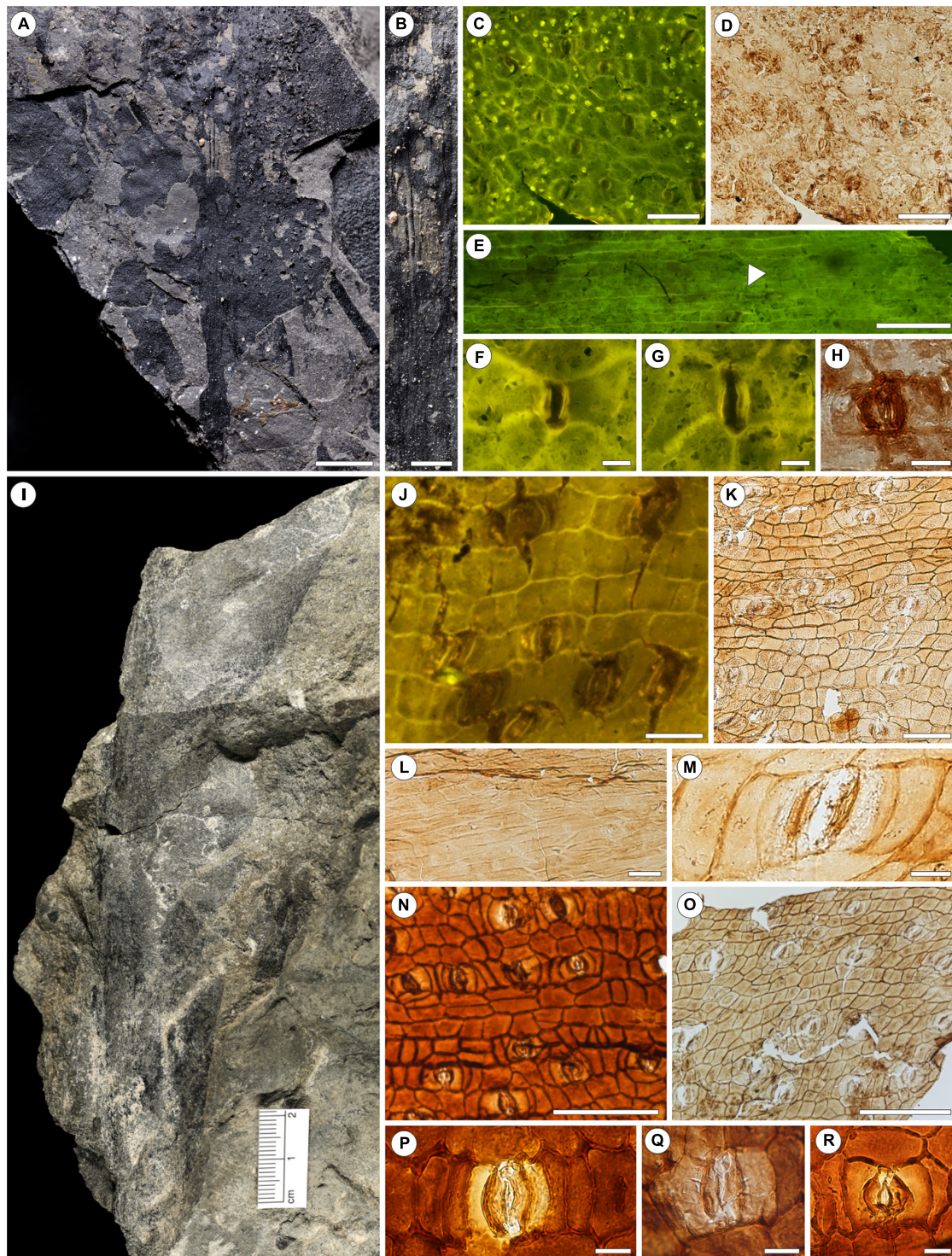


FIGURE 2 | *Nilssoniopteris jogiana* Blomenkemper et Abu Hamad sp. nov. from the upper Permian of Jordan (**A–G**) and *Nilssoniopteris shanxiensis* Bäumer, Backer et Wang sp. nov. from the lower Permian of China (**H–Q**). (**A**) Holotype of *N. jogiana* (Jo15-5-62) showing the partially preserved lamina and rachis. (**B**) Detail of (**A**) showing the striate rachis. (**C**) Lower leaf surface showing the costal field and unidentified organic particles. (**D**) Same section as **C** in transmitted light. (**E**) Upper surface of *N. jogiana*. Note the stoma (white arrow). (**F,G**) Epifluorescence image of typical stomata of *N. jogiana* from the lower leaf surface. (**H**) Typical stomata of *N. jogiana* in transmitted light. (**I**) Holotype of *N. shanxiensis* (PLG 137B-001). (**J**) *In situ* epifluorescence picture of the lower leaf surface (**H**). (**K**) Light microscopic image of the lower leaf surface. (**L**) Epidermal architecture of the rachis. Note the strongly elongate epidermal cells. (**M**) Detail of (**K**) showing a typical stoma of the lower leaf surface. (**N,O**) Lower (**N**) and upper (**O**) leaf surface. Note the difference in stomatal density. (**P–R**) Typical stomata of *N. shanxiensis*. Scale bars for (**A**) = 1 cm; (**B**) = 5 mm; (**C,D**) = 100 μm ; (**E**) = 200 μm ; (**F–H**) = 20 μm ; (**J**) = 50 μm ; (**K**) = 100 μm ; (**L**) = 50 μm ; (**M**) = 20 μm ; (**N,O**) = 200 μm ; (**P–R**) = 20 μm .

rectangular isodiametric; those in costal fields rectangular, slightly elongate, up to twice as long as wide (**Figure 2G**), some with faintly visible longitudinal striae on periclinal walls. All anticlinal walls of epidermal cells of the lower leaf surface smooth. Trichome bases are absent.

Upper surfaces nearly devoid of stomatal complexes (**Figure 2E**). Epidermal cells commonly strongly elongate, up to four times longer than wide, some with slightly undulating anticlinal walls.

Numerous organic particles present on all *in situ* cuticles of the lower surface (**Figure 2C**). These are of round to slightly ellipsoid shape, small, less than 10 μm in diameter, occasionally with faintly visible dent in central position.

Remarks and Comparisons

As there is no indication of a division of the leaf lamina, we presume it to be fully entire-margined similar to, e.g., *Nilssoniopteris angustior* (Pott et al., 2007b; Plate 3) or *N. vittata* (Harris, 1969; Figure 32A). *Nilssoniopteris jogiana* is easily delimited from most other species of *Nilssoniopteris* in having amphistomatic leaves (cf. Ray et al., 2014). *Nilssoniopteris jogiana* can easily be distinguished from species showing a similar leaf gross morphology, such as *N. vittata*, *N. major*, *N. pristis* (Harris, 1969), in having smooth anticlinal walls of the subsidiary and epidermal cells. From species showing similar smooth anticlinal walls, such as *N. haidingeri* (Pott et al., 2007b, Plate 2, **Figures 1–7**), it is delimited in being imperfectly amphistomatic and in lacking papillae, and from *N. angustior* (Pott et al., 2007b, Plate 4) in showing distinct costal and intercostal fields and in lacking papillae.

N. jogiana is delimited from the similarly amphistomatic *N. shanxiensis* (see below) by the presence of longitudinal striae on epidermal cells.

Nilssoniopteris shanxiensis Bäumler, Backer et Wang sp. nov.

Figures 2I–R

Diagnosis

Leaves large, simple, lamina entire-margined or irregularly divided into segments of unequal width. Insertion of lamina to rachis lateral; rachis prominent, lateral veins obliquely emerging from rachis, bifurcating basally. Leaf amphistomatic, with well-defined costal and intercostal fields on both surfaces; stomatal density lower on upper leaf surface. Stomata syndetocheilic, predominantly transversely oriented; epidermal cells with short papillae on the upper leaf surface; periclinal walls thickened or papillate on the lower leaf surface.

Holotype (Hic Designatus)

Partially preserved leaf (PLG 137B-001).

Additional Material

PC13701, PC13703–PC13714, PC13716, PC13718–PC13720, PC13724, PC13725, PC13802, PC13941, PC13942, PC13944, PC14194, PC14195 (*in situ*); PC13715, PC13721, PC13723, PC13726, PC13727, PC13803, PC14166 (bulk).

Type Locality

Palougou Section, Xiaohegou River valley, Shanxi Province, North China.

Type Stratum and Age

Uppermost part of Upper Shihhotse Formation Cisuralian (early Permian).

Etymology

The specific epithet is chosen in reference to the geographic occurrence of the type material.

Description

Leaves relatively large, at least 15 cm long by 4 cm wide (**Figure 2I**), simple. Leaf only partially preserved, presumably lanceolate. Leaf base and apex unknown, preserved leaf lamina entire-margined or irregularly subdivided into segments of unequal width, laterally inserted to rachis. Rachis prominent, longitudinally striated, up to 1.5 cm wide. Veins obliquely emerging from rachis at angles of 40° to 50°, bifurcating basally.

Leaf amphistomatic, costal, and intercostal fields well-developed on upper and lower leaf surfaces (**Figures 2J,K,N,O**), stomata confined to intercostal fields, trichome bases absent. Upper and lower leaf surfaces more or less similar, except for higher stomata density on the lower surface. Costal fields 140–190 μm , intercostal fields 180–260 μm wide on the lower leaf surface. Stomata randomly distributed, syndetocheilic, predominantly transversely oriented. Stomatal complexes up to 85 μm long, and 60 μm wide. Guard cells well cutinized. Subsidiary cells weakly cutinized (**Figure 2M**), frequently flanked by encircling cells (**Figures 2K,O**) and occasionally divided transversely. Ordinary cells in intercostal fields randomly oriented, polygonal-isodiametric, up to 45 μm in diameter. Epidermal cells in costal fields longitudinally oriented, rectangular, elongate to trapezoidal, up to 100 μm long and 35 μm wide. Anticlinal walls smooth and moderately thick. Periclinal walls papillate or thickened (**Figure 2N**).

Costal fields 130–180 μm wide, intercostal fields 160–240 μm wide on the upper leaf surface. Stomata confined to intercostal fields; density slightly lower than on lower leaf surface. Ordinary epidermal cells in intercostal fields polygonal-isodiametric up to 40 μm wide, ordinary epidermal cells in costal fields longitudinally oriented, polygonal-elongate or polygonal-isodiametric. Ordinary epidermal cells commonly with a central papilla. Anticlinal walls smooth, moderately thick.

Rachial areas distinct (**Figure 2L**), devoid of stomata and characterized by polygonal-elongate epidermal cells, up to 120 μm long, up to 30 μm wide. Anticlinal walls smooth and thin. Periclinal walls occasionally thickened.

Comparisons and Remarks

Nilssoniopteris shanxiensis is easily delimited from most other species of *Nilssoniopteris* in having amphistomatic leaves (cf. Ray et al., 2014). *Nilssoniopteris shanxiensis* is delimited from the similarly amphistomatic *N. jogiana* by its smooth periclinal walls of ordinary epidermal cells.

The stomatal architecture of this type is strikingly similar to that of *Nilssoniopteris angustior* illustrated by Pott et al.

(2007b). However, the overall epidermal anatomy shows distinct differences: (1) costal fields and intercostal fields are much more differentiated in the here described specimens, (2) unlike in *N. shanxiensis*, the upper leaf surface of *N. angustior* bears stomata only close to the rachis, (3) costal fields in *Nilssoniopteris angustior* have polygonal-elongate cells, similar to cells in intercostal fields.

Dispersed cuticles recovered from bulk material can be correlated with *in situ* cuticles by their epidermal anatomy and occur only in Bed 138 of the Upper Shihhotse Formation in the Palougou section. In a single specimen, epidermal cells and subsidiary cells are slightly more contracted.

Dispersed Bennettitalean Cuticles Recovered by Bulk Maceration

In addition to the hand specimens containing bennettitalean foliage remains described above, bulk maceration of samples from different localities of the Umm Irna Formation yielded six different types of bennettitalean cuticle fragments. We recognize that due to the fragmentary preservation of these dispersed cuticles information is limited, and we therefore refrain from a formal systematic treatment. However, since all fragments do show epidermal architecture that is diagnostic for the Bennettitales, including syndetocheilic stomata, they are informally described below in order to document the taxonomic diversity and variability in epidermal features among these Paleozoic members of the group.

Cuticle Type A

Figures 3A–C

Material

Three cuticle fragments (slides PaleoxyrisSiteBULKSL#011, #013–#014) from the Dyke Plateau, ~15 km south of the mouth of Wadi Zarqa Ma'in, along the eastern shore of the Dead Sea, Jordan.

Description

Lamina divided into costal and intercostal fields. Intercostal fields up to 300 μm wide; costal fields up to 100 μm wide. Ordinary epidermal cells within intercostal fields rectangular to polygonal, isodiametric with smooth anticlinal walls. Those in costal fields rectangular, slightly elongated but rarely being twice as long as wide. Stomatal complexes confined to the intercostal fields, here evenly spaced; comparatively small, not exceeding 60 μm in length and 40 μm in width. Stomatal pores narrow, predominantly transversely aligned; occasionally oriented longitudinally or obliquely. Lateral ledges of pores strongly cutinized.

Cuticle Type B

Figures 3D–F

Material

A single cuticle fragment (slide Roadcut4BSL#001) from the Dyke Plateau roadcut ~15 km south of the mouth of Wadi Zarqa Ma'in, along the eastern shore of the Dead Sea, Jordan.

Description

Lamina divided into costal and intercostal fields. Intercostal fields up to 300 μm wide; costal fields up to 80 μm wide. Ordinary epidermal cells within intercostal fields rectangular, isodiametric with smooth anticlinal walls. Those in costal fields elongate, up to three times as long as wide. Stomatal complexes evenly spaced, about up to 120 μm long and 40 μm , confined to the intercostal fields. Stomatal pores with strongly cutinized lateral ledges, oriented transversely.

Cuticle Type C

Figures 3G–I

Material

A single cuticle fragment (slide Roadcut4BSL#002) from the Dyke Plateau roadcut ~15 km south of the mouth of Wadi Zarqa Ma'in, along the eastern shore of the Dead Sea, Jordan.

Description

Lamina indistinctively divided into costal and intercostal fields. Epidermal cells in costal fields slightly more elongate, up to two times as long as wide, than those in intercostal fields. Ordinary epidermal cells in intercostal fields, isodiametric and, by contrast, with distinct sinuous anticlinal walls. Stomatal complexes confined to intercostal fields, stomatal pores transversely oriented, with strongly cutinized lateral ledges. Subsidiary cells stronger cutinized than surrounding epidermal cells and with smooth anticlinal walls.

Remarks

Due to low density of stomatal complexes and indistinctive costal and intercostal fields we interpret this fragment to likely represent the upper surface.

Cuticle Type D

Figures 3J–L

Material

A single cuticle fragment (slide Roadcut4BSL#004) from the Dyke Plateau roadcut ~15 km south of the mouth of Wadi Zarqa Ma'in, along the eastern shore of the Dead Sea, Jordan.

Description

Lamina divided into costal and intercostal fields. Intercostal fields up to 250 μm wide; costal fields up to 50 μm wide. Ordinary epidermal cells in intercostal fields isodiametric to elongate, up to twice as long as wide; anticlinal walls sinuous, periclinal walls commonly with distinct, randomly oriented striae. Costal fields consisting of ordinary, rectangular, elongate epidermal cells, up to four times long as wide; anticlinal walls sinuous, periclinal walls smooth. Stomatal complexes up to 90 μm long and 30 μm wide, confined to intercostal fields, loosely spaced. Stomatal pores with strongly cutinized lateral ledges, predominantly transversely aligned, rarely oriented longitudinally or obliquely; occasionally with four subsidiary cells resulting from further transverse division of subsidiary cells. Anticlinal walls of subsidiary cells smooth.

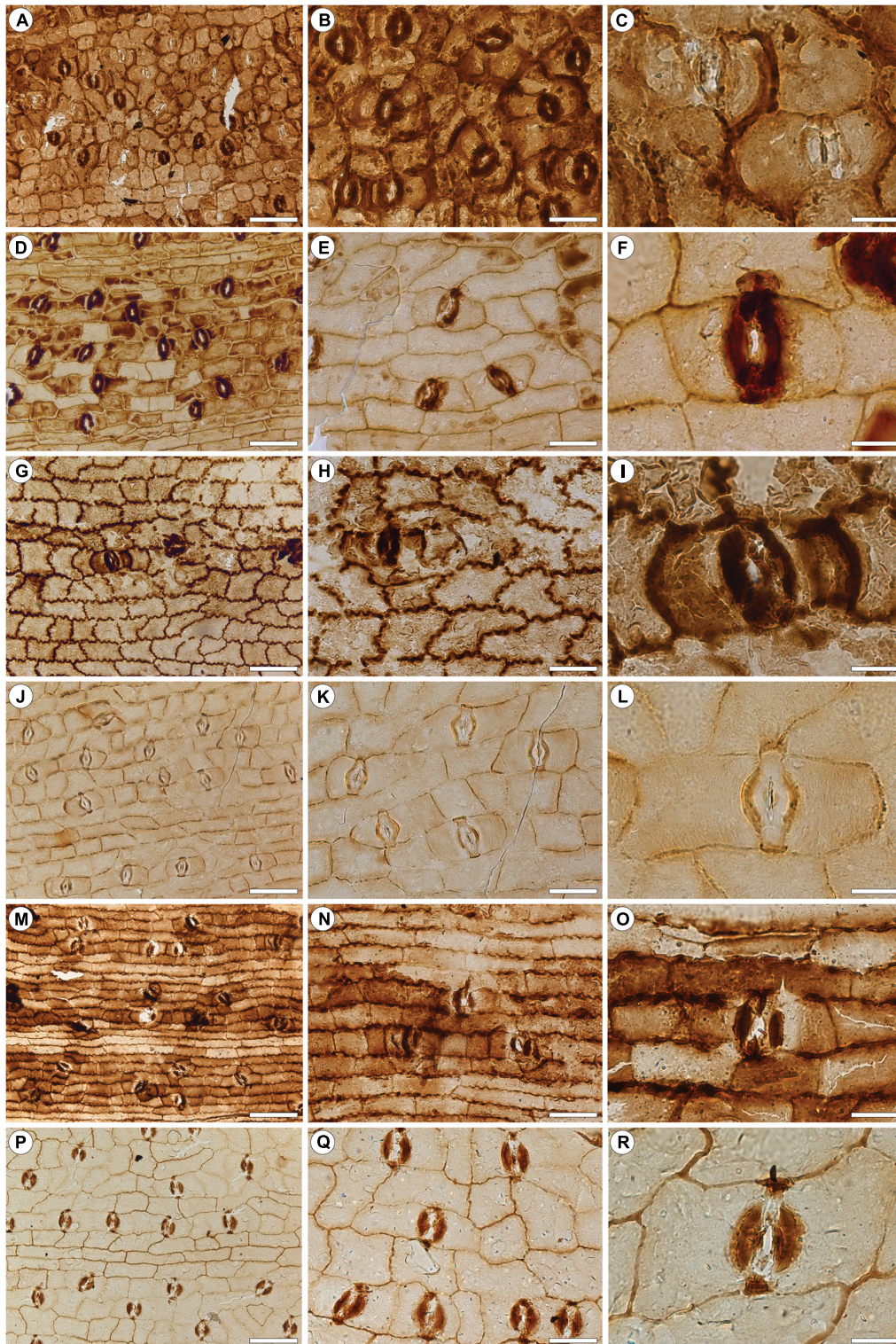


FIGURE 3 | Dispersed bennettitalean cuticles recovered by bulk maceration from the upper Permian of Jordan. Type A (A–C); Type B (D–F); Type C (G–I); Type D (J–L); Type E (M–O); Type F (P–R). (A) Presumed lower leaf surface. (B) Detail of (A) showing the costal field. (C) Typical stomata. (D) Presumed lower leaf surface. (E) Detail of (D) showing the costal field. (F) Typical stoma. (G) Presumed upper surface. Note the comparatively strongly sinuous anticlinal walls. (H) Detail of (G). (I) Typical stoma. (J) Presumed lower leaf surface. (K) Detail of (J) showing a costal field. (L) Typical stoma. (M) Presumed lower leaf surface. Note the comparatively strongly elongate epidermal cells in intercostal fields and sinuate anticlinal walls. (N) Detail of (M) showing the costal field. (O) Typical stoma. (P) Presumed lower leaf surface. (Q) Detail of (P) showing the costal field. Note the slightly sinuate epidermal cells within the costal field. (R) Typical stoma. Scale bars for (A,D,G,J,M,P) = 100 μm ; (B,E,H,K,N,Q) = 50 μm ; (C,F,I,L,O,R) = 20 μm .

Cuticle Type E

Figures 3M–O

Material

A single cuticle fragment (slide PaleoxyrisSiteSL#015) from the Dyke Plateau ~15 km south of the mouth of Wadi Zarqa Ma'in, along the eastern shore of the Dead Sea, Jordan.

Description

Lamina divided into distinct costal and intercostal fields. Intercostal fields up to 300 μm wide; costal fields up to 100 μm wide. Ordinary epidermal cells in intercostal fields polygonal isodiametric to slightly elongate, up to twice as long as wide, longitudinally or rarely transversely oriented. Costal fields consisting of isodiametric to rectangular-elongate epidermal cells, the latter being up to three times as long as wide. Anticlinal walls slightly undulate. Stomatal complexes about up to 130 μm long and 50 μm wide, confined to the intercostal fields, closely spaced, some sharing subsidiary cells, or with much smaller subsidiary cells between closely spaced complexes. Stomatal pores oriented transversely with strongly cutinized lateral ledges and polar knobs.

Cuticle Type F

Figures 3P–R

Material

A single cuticle fragment (slide Roadcut4BSL#003) from the Dyke Plateau roadcut ~15 km south of the mouth of Wadi Zarqa Ma'in, along the eastern shore of the Dead Sea, Jordan.

Description

Lamina divided into costal and intercostal fields. Intercostal fields imperfectly preserved; costal fields up to 50 μm wide. Ordinary epidermal cells within intercostal fields rectangular, isodiametric with smooth anticlinal cell walls. Those in costal fields elongate, up to three times long as wide, anticlinal walls smooth; some periclinal walls with faintly visible, longitudinal striae. Stomatal complexes about up to 100 μm long and 40 μm wide, confined to intercostal fields, evenly spaced. Stomatal pores with small, strongly cutinized ledges and knobs, mostly oriented transversely, rarely perpendicularly or obliquely.

DISCUSSION

The here described material represents the oldest bennettitalean foliage that can be unambiguously identified based on diagnostic epidermal features. Tracking the evolutionary history of the Bennettitales and other gymnosperm groups through Earth's history is hampered by the incompleteness of the fossil record, particularly the rareness of floras from extrabasinal environments where these groups apparently appeared first (e.g., Falcon-Lang et al., 2009; Looy et al., 2014; Blomenkemper et al., 2018). Especially for Bennettitales, cuticle preservation is crucial. Bennettitalean and cycadalean leaves can be very similar and can often only be distinguished on the basis of their epidermal

architecture, notably the morphology of the stomatal complexes (Florin, 1933).

Several cycad-like leaf types have been reported from uppermost Carboniferous and Permian strata of Euramerica, Angara, and Cathaysia and some have even been assigned to fossil genera for bennettitalean foliage, such as *Pterophyllum*. For a comprehensive, critical review of 21 late Paleozoic species assigned to *Pterophyllum* we refer to Pott et al. (2009), although a few remarks should be made. *Pterophyllum gonorrhachis* (Göppert, 1844) does not show the typical segmented leaf architecture; the irregular appearance and the scars on the surface of the axis suggest that it is a root. Although Zeiller (1906) cites de Saporta and Marion (1885) as the authors of *Pterophyllum grandeuryi*, the specimen he described from Blanzky (France) has long, broadly attached, decurrent leaf segments, whereas *Pterophyllum grandeuryanum* illustrated by Saporta and Marion has rather short, obovate, basally constricted leaf segments. The age of the material from the Commentry and Blanzky basins is Stephanian, late Carboniferous.

Cuticles from foliage from Shanxi, China, originally assigned to *Pterophyllum samchokense* (Kawasaki, 1934), revealed that these leaves were of cycadalean rather than of bennettitalean affinity (Pott et al., 2009); consequently, the species was transferred to *Pseudoctenis*. Similarly, several species from the Upper Triassic of Lunz (Austria), originally assigned to *Pterophyllum*, appeared to be of cycadalean instead of bennettitalean affinity (Pott et al., 2007a,b). These examples illustrate how difficult it is to classify cycad-like leaves without having information on the epidermal anatomy.

Careful analysis of the cuticles of cycad-like leaves from the Permian of China and Jordan resulted in the recognition of three new species of early Bennettitales, a group of which the oldest putative representatives have so far been reported from the Middle Triassic (Wachtler and Van Konijnenburg-van Cittert, 2000; Kustatscher and Van Konijnenburg-van Cittert, 2005; McLoughlin et al., 2018). *Nilssoniopteris shanxiensis* from the Cisuralian of Shanxi is the oldest known *bona fide* bennettitalean. The genus *Nilssoniopteris* (Nathorst, 1909) is used for simple taeniopterid to irregularly lobed foliage with bennettitalean epidermal architecture (e.g., Harris, 1969; Boyd, 2000; Pott et al., 2007b). The somewhat younger *Nilssoniopteris jogiana* from the uppermost Permian of Jordan is another late Paleozoic species assignable to this genus. The third species is *Pterophyllum pottii*, also from the uppermost Permian of Jordan. Bulk macerations of samples from Jordan revealed no less than six different types of bennettitalean cuticles. These cannot be assigned to any known genus due to the lack of information on the leaf morphology. Nevertheless, the morphology of the stomata leaves no doubt that they are of bennettitalean affinity. Together, the material from China and Jordan demonstrates that the Bennettitales, although never really common, were already widely distributed within the paleoequatorial belt by the end of the Permian (see **Figure 4**; see Torsvik and Cocks, 2016).

In addition to the above-mentioned *Pterophyllum* species, there is a whole array of species of cycad-like foliage that are all based on compressions without cuticle from the uppermost

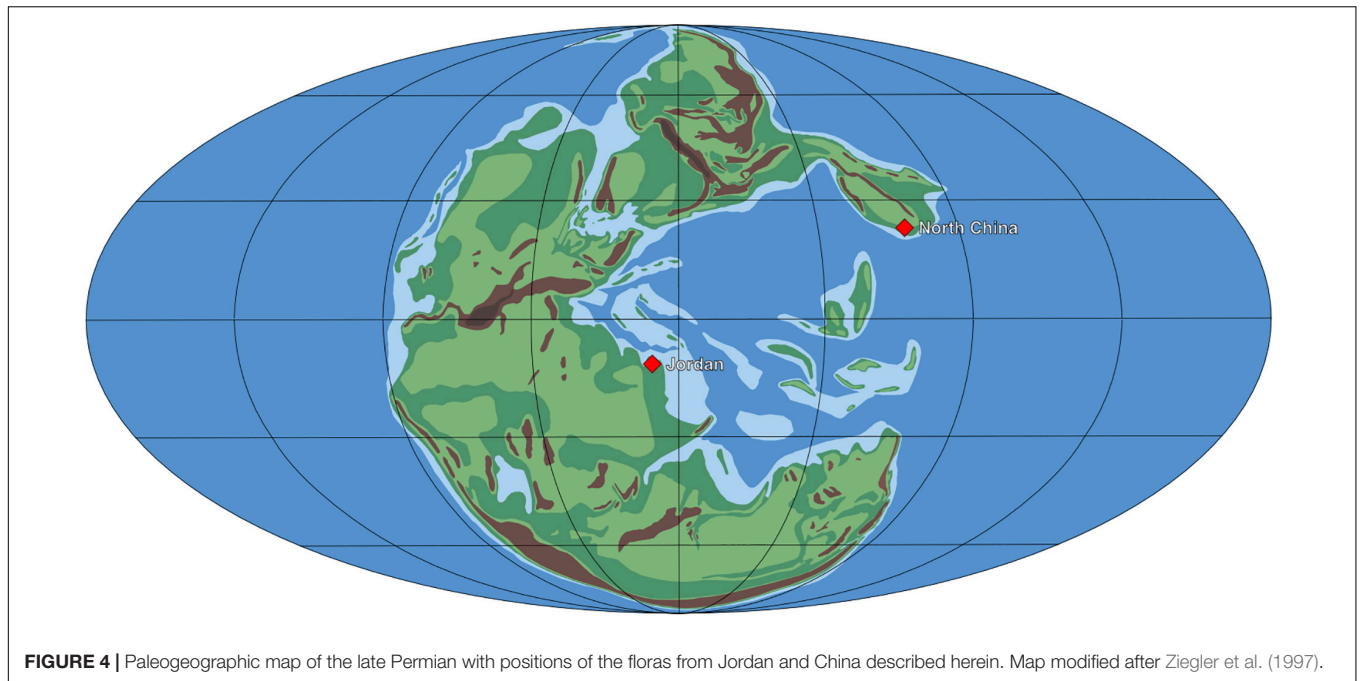


FIGURE 4 | Paleogeographic map of the late Permian with positions of the floras from Jordan and China described herein. Map modified after Ziegler et al. (1997).

Carboniferous and Permian of the Northern Hemisphere, notably from China. These have been assigned to genera like *Plagiozamites* (Zeiller, 1894; Bassler, 1916; Halle, 1927) and *Nilssonia* (Yang et al., 2006). With the exception of *Pseudoctenis samchokense* (Kawasaki) (Pott et al., 2009) from the lower Permian of South Korea, Shanxi and Guangdong (China), and *Plagiozamites oblongifolius* (Halle, 1927) from the lower Permian of Shanxi and Yunnan, which both appeared to be of cycadalean affinity (Pott et al., 2009; Feng et al., 2017), the natural relationships of the remaining foliage types are still unclear and can only be clarified when specimens with cuticle preservation become available. It can even not be excluded that some of these leaf types belong to the Noeggerathiales, a peculiar group of Carboniferous–Permian pteridophytes with a very disjunct distribution, geographically as well as stratigraphically. This group has superficially similar leaves (e.g., Wang et al., 2020), with very simple stomata (Liu et al., 1998; Šimůnek and Bek, 2003).

It may safely be assumed that apart from *Pseudoctenis samchokense* and *Plagiozamites oblongifolius* more of such leaf species belong to the Cycadales, regarding the fact that quite a number of typical cycadalean megasporophylls have been described from the lower Permian of China (Gao and Thomas, 1989; Yang et al., 2006). Four species showing a remarkable similarity to sporophylls of modern cycads were assigned to *Crossozamia* (Gao and Thomas, 1989), and two others were described as *Primozamia* and *Liella* (Yang et al., 2006). However, it should be considered that some early cycads had taeniopterid leaves (Florin, 1933). The natural affinities of the presumed early cycads from the lower Permian of Texas described by Mamay (1976) remain unclear; *Phasmatoxycas* appears to be a *Spermopteris*-like pteridosperm (Axsmith et al., 2003). The most convincing early cycad fossil from

Euramerica is *Dioonitocarpidium* from the lower Permian of Texas (DiMichele et al., 2001).

Although their natural relationship is still unclear, Cycadales and Bennettitales both evolved around the same time and first appeared in seasonally dry environments in paleoequatorial regions. Cycads and many Bennettitales have the same growth form, a trunk-like, rarely branched or unbranched stem bearing a crown of stiff, leather-like leaves. This growth habit was highly successful as both were among the dominant plant groups during most of the Mesozoic.

The here described late Paleozoic Bennettitales of China and Jordan apparently preferred similar habitats. The material from China was collected from fluvial deposits intercalated into otherwise barren redbeds (e.g., Liu et al., 2015) and that from Jordan from similar, fluvial environments that were influenced by seasonal drought in a monsoonal climate (Kerp et al., 2006; Abu Hamad et al., 2008; Stephenson and Powell, 2013). Adaptation to these disturbance-prone environments may have played a key role in the ability of the plants to cope with the dramatic changes in the course of the Permian–Triassic transition and their success during the Triassic and Jurassic. Unlike highly competitive groups preferring stable humid conditions, such as gigantopterids and glossopterids that vanish from the fossil record at or shortly after the P/T boundary, Bennettitales thrived throughout the Triassic reaching a global distribution during the Late Triassic, similar to other groups whose earliest *bona fide* records, i.e., the *Corystospermales* and podocarpacean conifers, have been documented from these environments (Abu Hamad et al., 2008; Blomenkemper et al., 2018, 2020). The Bennettitales and other plants growing in periodically drier environments show a remarkable resilience toward the dramatic turnovers (Bomfleur et al., 2018) that affected the terrestrial and marine fauna so strongly (e.g., Erwin, 1999; Sahney and Benton, 2008).

The cuticles of here described early Bennettitales and their Mesozoic relatives both show a clear differentiation into costal and intercostal fields with syndetocheilic stomata. Anticlinal walls of late Paleozoic Bennettitales, however, are mostly straight or finely sinuous, whereas those of Mesozoic forms often are strongly undulating. A similar pattern can be seen in some members of the genus *Dicroidium* (cf. Townrow, 1957; Anderson and Anderson, 1983; Abu Hamad et al., 2008; Bomfleur and Kerp, 2010). Whether this was an adaptation to changing environmental conditions, an evolutionary trend, or a combination of both is still unclear.

Taking the wide distribution of late Paleozoic Bennettitales and their diversity, including the variety of cuticle types from bulk macerations, into account, it is obvious that this group must have evolved much earlier. Also, here we see a striking parallel with the *Corystospermales*, which already show a great diversity during the late Permian, albeit not in their “classical” Triassic distribution range in southern Gondwana. For plants growing outside peat-forming environments, the Permian can be seen as the dawn of the Mesozoic rather than the end of an era.

DATA AVAILABILITY STATEMENT

The original contributions presented in the study are included in the article/supplementary material, further inquiries can be directed to the corresponding author/s.

AUTHOR CONTRIBUTIONS

PB, RB, and MB prepared, analyzed, and documented the material. AAH and JW organized field work. PB, HK, and BB contributed to initial manuscript preparation. HK and BB conceived the project. All authors contributed to field

work, to discussion and to final manuscript preparation, and approved submission.

FUNDING

Financial support was provided by the German Research Foundation (Deutsche Forschungsgemeinschaft, DFG) Emmy Noether grant BO 3131/1-1 “Latitudinal Patterns in Plant Evolution” to BB, grants KE 584/20-1 and KE 584/21-1 to HK, and by the Chinese Academy of Sciences and the Nanjing Institute for Geology and Paleontology. This article was also result of the Chinese–German joint project “Late Paleozoic Paleobiology, Stratigraphy and Geochemistry” (GZ575) coordinated by Wang Xiandong and HK, funded by the Sino-German Center for Research Promotion (Beijing), a cooperation of the National Natural Science Foundation of China and the German Research Foundation.

ACKNOWLEDGMENTS

We thank the editors, especially EK and Robert A. Gastaldo, for the invitation to contribute to this Special Topic article collection and for kind and swift editorial handling. Liu Feng, Zhou Weiming, Wan Mingli, Mei Shengwu, and Wei Hai-Bo for fieldwork assistance in China and collection studies in the Nanjing Institute for Geology and Paleontology. Haatem S. Badandi, Nidal S. Badandi, Yahia S. Badandi, Jörg “Jogi” Schneider, Frank Scholze, and Sebastian Voigt for fieldwork assistance in Jordan. Christian Pott for helpful discussion; and Anne Niehus for assistance in chemical preparation. We would also like to thank WD and MP for their constructive reviews.

REFERENCES

- Abu Hamad, A., Blomenkemper, P., Kerp, H., and Bomfleur, B. (2017). *Dicroidium bandelii* sp. nov. (corystospermalean foliage) from the Permian of Jordan. *PalZ* 91, 641–648. doi: 10.1007/s12542-017-0384-2
- Abu Hamad, A., Fischer, J., Voigt, S., Kerp, H., Schneider, J. W., and Scholze, F. (2016). First Permian occurrence of the shark egg capsule morphotype *Palaeoxyris* Brongniart, 1828. *J. Vertebr. Paleontol.* 36:e1112290. doi: 10.1080/02724634.2016.1112290
- Abu Hamad, A., Kerp, H., Vörding, B., and Bandel, K. (2008). A late Permian flora with *Dicroidium* from the Dead Sea region. *Rev. Palaeobot. Palynol.* 149, 85–130. doi: 10.1016/j.revpalbo.2007.10.006
- Anderson, J., Anderson, H., Fatti, P., and Sichel, H. (1996). The Triassic Explosion(?): a statistical model for extrapolating biodiversity based on the terrestrial Molteno Formation. *Paleobiology* 22, 318–328. doi: 10.1017/S0094837300016304
- Anderson, J. M., and Anderson, H. M. (1983). *Palaeoflora of Southern Africa—Molteno Formation, Volume 1, Part 1—Introduction/Part 2—Dicroidium*. Rotterdam: Balkema.
- Axsmith, B. J., Serbet, R., Krings, M., Taylor, T. N., Taylor, E. L., and Mamay, S. H. (2003). The enigmatic Paleozoic plants *Spermopteris* and *Phasmatocycas* reconsidered. *Am. J. Bot.* 90, 1585–1595. doi: 10.3732/ajb.90.11.1585
- Bandel, K., and Khoury, H. (1981). Lithostratigraphy of the Triassic in Jordan. *Facies* 4, 1–26. doi: 10.1007/BF02536584
- Bassler, H. (1916). A cycadophyte from the North American coal measures. *Am. J. Sci.* s4-42, 21–26. doi: 10.2475/ajs.s4-42.247.21
- Bernardi, M., Petti, F. M., Kustatscher, E., Franz, M., Hartkopf-Fröder, C., Labandeira, C. C., et al. (2017). Late Permian (Lopingian) terrestrial ecosystems: a global comparison with new data from the low-latitude Bletterbach Biota. *Earth-Sci. Rev.* 175, 18–43. doi: 10.1016/j.earscirev.2017.10.002
- Blomenkemper, P., Abu Hamad, A., and Bomfleur, B. (2019). *Cryptokerpia sarlaccophora* gen. et sp. nov., an enigmatic plant fossil from the Late Permian Umm Irna Formation of Jordan. *PalZ* 93, 479–485. doi: 10.1007/s12542-019-00466-x
- Blomenkemper, P., Kerp, H., Abu Hamad, A., and Bomfleur, B. (2020). Contributions towards whole-plant reconstructions of *Dicroidium* plants (Umkomasiaceae) from the Permian of Jordan. *Rev. Palaeobot. Palynol.* 278:104210. doi: 10.1016/j.revpalbo.2020.104210
- Blomenkemper, P., Kerp, H., Abu Hamad, A., DiMichele, W. A., and Bomfleur, B. (2018). A hidden cradle of plant evolution in Permian tropical lowlands. *Science* 362, 1414–1416. doi: 10.1126/science.aau4061
- Bomfleur, B., Blomenkemper, P., Kerp, H., and McLoughlin, S. (2018). “Polar Regions of the Mesozoic–Paleogene Greenhouse World as Refugia for Relict Plant Groups,” in *Transformative Palaeobotany*, eds M. Krings, C. J. Harper, N. R. Cúneo, and G. W. Rothwell (Amsterdam: Academic Press), 593–611. doi: 10.1016/B978-0-12-813012-4.00024-3

- Bomfleur, B., and Kerp, H. (2010). *Dicroidium* diversity in the Upper Triassic of north Victoria land, East Antarctica. *Rev. Palaeobot. Palynol.* 160, 67–101. doi: 10.1016/j.revpalbo.2010.02.006
- Boy, A. (2000). Bennettitales from the Early Cretaceous floras of West Greenland: *Pterophyllum* and *Nilssoniopteris*. *Palaeontographica B* 255, 47–77. doi: 10.1127/palb/255/2000/47
- Brongniart, A. (1825). Observations sur les végétaux fossils renfermés dans les Grès de Hoer en Scanie. *Ann. Sci. Nat.* 4, 200–224.
- Cleal, C. J., and Rees, P. M. (2003). The Middle Jurassic flora from Stonesfield, Oxfordshire, UK. *Palaeontology* 46, 739–801. doi: 10.1111/1475-4983.00319
- de Saporta, G., and Marion, A.-F. (1885). *L'évolution du Règne Végétal - Les Phanérogames, Tome Premier*. Paris: Félix Alcan.
- DiMichele, W. A., Mamay, S. H., Chaney, D. H., Hook, R. W., and Nelson, W. J. (2001). An Early Permian flora with Late Permian and Mesozoic affinities from north-central Texas. *J. Paleont.* 75, 449–460. doi: 10.1017/S002233600018230
- Engler, A. (1892). *Syllabus der Vorlesungen Über Spezielle und Medicinisch-Pharmaceutische Botanik*. Berlin: Gebr. Borntraeger. doi: 10.5962/bhl.title.69853
- Erwin, D. (1993). *The Great Paleozoic Crisis. Life and Death in the Permian*. New York, NY: Columbia University Press.
- Erwin, D. (1999). Biospheric perturbations during Gondwanan times. from the Neoproterozoic–Cambrian radiation to the end-Permian crisis. *J. Afr. Earth Sci.* 28, 115–127. doi: 10.1016/S0899-5362(99)00021-4
- Falcon-Lang, H. J., Nelson, W. J., Elrick, S., Looy, C. V., Ames, P. R., and DiMichele, W. A. (2009). Incised channel fills containing conifers indicate that seasonally dry vegetation dominated Pennsylvanian tropical lowlands. *Geology* 37, 923–926. doi: 10.1130/G30117A.1
- Feng, Z., Yong, L., Yun, G., Hai-Bo, W., and Kerp, H. (2017). Leaf anatomy of a late Palaeozoic cycad. *Biol. Lett.* 13:1320170456. doi: 10.1098/rsbl.2017.0456
- Florin, R. (1933). Studien über die Cycadales des Mesozoikums nebst Erörterungen über die Spaltöffnungsapparate der Bennettitales. *Kunl. Svenska Vetenskapsakad. Handl.* 12, 1–134.
- Gao, Z., and Thomas, B. A. (1989). A review of fossil cycad megasporophylls, with new evidence of *Crossozamia* Pomel and its associated leaves from the Lower Permian of Taiyuan, China. *Rev. Palaeobot. Palynol.* 60, 205–223. doi: 10.1016/0034-6667(89)90044-4
- Göppert, H. R. (1844). Ueber die fossilen Cykadeen überhaupt, mit Rücksicht auf die in Schlesien vorkommenden Arten. *Uebersicht der Arbeiten und Veränderungen der schlesischen Gesellschaft für vaterländische Kultur*. 1844, 114–144.
- Grebe, H. (1956). Zur Mikroflora des niederrheinischen Zechsteins. *Z. Dtsch. Geol. Ges.* 108, 234–269.
- Grebe, H., and Schweitzer, H.-J. (1962). Die Sporeae dispersae des niederrheinischen Zechsteins. *Fortschr. Geol. Rheinl. Westf.* 12, 1–24.
- Halle, T. G. (1927). Palaeozoic Plants from Central Shansi. *Palaeontol. Sin. Ser. A.2*, 1–316.
- Harris, T. M. (1969). *The Yorkshire Jurassic Flora III. Bennettitales*. London: Trustees of the British Museum (Natural History).
- Hochuli, P. A., Vigran, J. O., Hermann, E., and Bucher, H. (2010). Multiple climatic changes around the Permian–Triassic boundary event revealed by an expanded palynological record from mid-Norway. *GSA Bull.* 122, 884–896. doi: 10.1130/B26551.1
- Kawasaki, S. (1934). The flora of the Heian System—Part 2. *Bull. Geol. Surv. Chosen (Korea)* 6, 47–311.
- Kerp, H. (1990). The Study of Fossil Gymnosperms by Means of Cuticular Analysis. *Palaiois* 5, 548–569. doi: 10.2307/3514861
- Kerp, H., Abu Hamad, A., Vörding, B., and Bandel, K. (2006). Typical Triassic Gondwanan floral elements in the Upper Permian of the paleotropics. *Geology* 34, 265–268. doi: 10.1130/G22187.1
- Kerp, H., and Bomfleur, B. (2011). Photography of plant fossils—New techniques, old tricks. *Rev. Palaeobot. Palynol.* 166, 117–151. doi: 10.1016/j.revpalbo.2011.05.001
- Krings, M., and Kerp, H. (1997). An improved method for obtaining large pteridosperm cuticles. *Rev. Palaeobot. Palynol.* 96, 453–456. doi: 10.1016/S0034-6667(96)00059-0
- Kustatscher, E., and Van Konijnenburg-van Cittert, J. H. A. (2005). The Ladinian flora (Middle Triassic) of the Dolomites: palaeoenvironmental reconstructions and palaeoclimatic considerations. *Geo. Alp* 2, 31–51.
- Liu, F., Zhu, H. C., and Ouyang, S. (2015). Late Pennsylvanian to Wuchiapingian palynostratigraphy of the Baode section in the Ordos Basin, North China. *J. Asian Earth Sci.* 111, 528–552. doi: 10.1016/j.jseas.2015.06.013
- Liu, Z.-H., Geng, B.-Y., Cui, J.-Z., and Li, C.-S. (1998). Studies on the Epidermal Structure of *Tingia carbonica*. *J. Syst. Evol.* 36, 341–345.
- Looy, C., Kerp, H., Duijnste, I., and DiMichele, W. A. (2014). The late Paleozoic ecological-evolutionary laboratory, a land-plant fossil record perspective. *Sedimentary Rec.* 12, 4–18. doi: 10.2110/sedred.2014.4.4
- Mamay, S. H. (1976). Paleozoic origin of the cycads. *U.S. Geol. Surv. Prof. Pap.* 934, 1–48. doi: 10.3133/pp934
- McLoughlin, S., Pott, C., and Sobbe, I. H. (2018). The diversity of Australian Mesozoic bennettitoid reproductive organs. *Palaeobiodiv. Palaeoenvironm.* 98, 71–95. doi: 10.1007/s12549-017-0286-z
- Mustafa, H. (2003). A late Permian Cathaysia flora from the Dead Sea area, Jordan. *N. Jb. Geol. Paläont. Mh.* 2003, 35–39. doi: 10.1127/njgpm/2003/2003/35
- Nathorst, A. G. (1909). Über die Gattung *Nilssonia* Brongn. *Kunl. Svenska Vetenskapsakad. Handl.* 43, 3–37.
- Nowak, H., Mette, W., Petti, F. M., Roghi, G., and Kustatscher, E. (2019). Palynology, microfacies and ostracods of the Permian–Triassic boundary interval in the Rosengarten/Catinaccio Massif (Southern Alps, Italy). *Austrian J. Earth Sci.* 112, 103–124. doi: 10.17738/ajes.2019.0007
- Ouyang, S., and Utting, J. (1990). Palynology of Upper Permian and Lower Triassic rocks, Meishan, Changxing County, Zhejiang Province, China. *Rev. Palaeobot. Palynol.* 66, 65–103. doi: 10.1016/0034-6667(90)90029-1
- Peng, Y., Yu, J., Gao, Y., and Yang, F. (2006). Palynological assemblages of non-marine rocks at the Permian–Triassic boundary, western Guizhou and eastern Yunnan, South China. *J. Asian Earth Sci.* 28, 291–305. doi: 10.1016/j.jseas.2005.10.007
- Phillips, J. (1829). *Illustrations of the Geology of Yorkshire; or, a Description of the Strata and Organic Remains of the Yorkshire Coast: Accompanied by a Geological Map, Sections, and Plates of the Fossil Plants and Animals*. New York, NY: Thomas Wilson & Sons. doi: 10.5962/bhl.title.30592
- Pott, C., Krings, M., and Kerp, H. (2007a). A surface microrelief on the leaves of *Glossophyllum florinii* (?Ginkgoales) from the Upper Triassic of Lunz, Austria. *Bot. J. Linn. Soc.* 153, 87–95. doi: 10.1111/j.1095-8339.2007.00569.x
- Pott, C., Krings, M., and Kerp, H. (2007b). First record of *Nilssoniopteris* (Gymnospermyta, Bennettitales) from the Carnian (Upper Triassic) of Lunz, Lower Austria. *Palaeontology* 50, 1299–1318. doi: 10.1111/j.1475-4983.2007.00704.x
- Pott, C., Van Konijnenburg-van Cittert, J. H. A., Kerp, H., and Krings, M. (2007c). Revision of the *Pterophyllum* species (Cycadophytina: Bennettitales) in the Carnian (Late Triassic) flora from Lunz, Lower Austria. *Rev. Palaeobot. Palynol.* 147, 3–27. doi: 10.1016/j.revpalbo.2007.03.005
- Pott, C., McLoughlin, S., and Lindström, A. (2009). Late Palaeozoic foliage from China displays affinities to Cycadales rather than to Bennettitales necessitating a re-evaluation of the Palaeozoic *Pterophyllum* species. *Acta Palaeontol. Pol.* 55, 157–168. doi: 10.4202/app.2009.0070
- Pott, C., Schmeißner, S., Dütsch, G., and Van Konijnenburg-van Cittert, J. H. A. (2016). Bennettitales in the Rhaetian flora of Wüstenwelsberg, Bavaria, Germany. *Rev. Palaeobot. Palynol.* 232, 98–118. doi: 10.1016/j.revpalbo.2016.04.010
- Powell, J. H., Nicora, A., Perri, M. C., Rettori, R., Posenato, R., Stephenson, M. H., et al. (2019). Lower Triassic (Induan to Olenekian) condonts, foraminifera and bivalves from the Al Mamalih area, Dead Sea, Jordan: Constraints on the P-T boundary. *Riv. Ital. di Paleontol. e Stratigr.* 125, 147–181.
- Powell, J. H., Stephenson, M. H., Nicora, A., Rettori, R., Borlenghi, L. M., and Perri, M. C. (2016). The Permian–Triassic boundary, Dead Sea, Jordan: Transitional alluvial to marine depositional sequences and biostratigraphy. *Riv. Ital. di Paleontol. e Stratigr.* 122, 23–40.
- Ray, M. M., Rothwell, G. W., and Stockey, R. A. (2014). Anatomically preserved Early Cretaceous bennettitalean leaves: *Nilssoniopteris corrugata* n. sp. from Vancouver Island. *Canada. J. Paleontol.* 88, 1085–1093. doi: 10.1666/13-108
- Sahney, S., and Benton, M. (2008). Recovery from the most profound mass extinction of all time. *Proc. R. Soc. B* 275, 759–765. doi: 10.1098/rspb.2007.1370
- Schneebeil-Hermann, E., Hochuli, P. A., and Bucher, H. (2017). Palynofloral associations before and after the Permian–Triassic mass extinction, Kap Stosch, East Greenland. *Global. Planet. Change* 155, 178–195. doi: 10.1016/j.gloplacha.2017.06.009

- Schneebeli-Hermann, E., Kürschner, W. M., Kerp, H., Bomfleur, B., Hochuli, P. A., Bucher, H., et al. (2015). Vegetation history across the Permian-Triassic boundary in Pakistan (Amb section, Salt Range). *Gondwana Res.* 27, 911–924. doi: 10.1016/j.gr.2013.11.007
- Šimůnek, Z., and Bek, J. (2003). Noeggerathiaceae from the Carboniferous basins of the Bohemian Massif. *Rev. Palaeobot. Palynol.* 125, 249–284. doi: 10.1016/S0034-6667(03)00004-6
- Schlothem, E. F. V. (1822). *Nachträge zur Petrefactenkunde*. Gotha: Becker'sche Verlagsbuchhandlung.
- Stephenson, M. H., and Powell, J. H. (2013). Palynology and alluvial architecture in the Permian Umm irna Formation, Dead Sea, Jordan. *GeoArabia* 18, 17–60.
- Thomas, H. H., and Bancroft, N. (1913). On the cuticles of some recent and fossil cycadean fronds. *Trans. Linn. Soc. Ser. 2 Bot.* 8, 155–204. doi: 10.1111/j.1095-8339.1913.tb00284.x
- Torsvik, T., and Cocks, L. (2016). *Earth History and Palaeogeography*. Cambridge: Cambridge University Press. doi: 10.1017/9781316225523
- Townrow, J. A. (1957). On *Dicroidium*, probably a pteridospermous leaf, and other leaves now removed from this genus. *South Afr. J. Geol.* 60, 1–60.
- Wachtler, M., and Van Konijnenburg-van Cittert, J. H. A. (2000). The fossil flora of the Wengen Formation (Ladinian) in the Dolomites (Italy). *Beitr. Paläont.* 25, 105–141.
- Wang, J., Wan, S., Kerp, H., Bek, J., and Wang, S. (2020). A whole noeggerathialean plant *Tingia unita* Wang from the earliest Permian peat-forming flora, Wuda Coalfield, Inner Mongolia. *Rev. Palaeobot. Palynol.* 104204. doi: 10.1016/j.revpalbo.2020.104204
- Watson, J., and Sincock, C. A. (1992). *Bennettitales of the English Wealden*. London: The Palaeontographical Society.
- Wu, Q., Ramezani, J., Zhang, H., Wang, J., Zeng, F., Zhang, Y., et al. (2021). High-precision U-Pb age constraints on the Permian floral turnovers, paleoclimate change, and tectonics of the North China block. *Geology* doi: 10.1130/G48051.1
- Yang, G. X., Wang, H. S., Zeng, X. L., and Xie, J. H. (2006). *The Permian Cathaysian Flora in Western Henan Province, China — Yuzhou Flora*. Beijing: Geology Publishing House. (in Chinese).
- Yin, H.-F., Yang, F.-Q., Yu, J.-X., Peng, Y.-Q., Wang, S. Y., and Zhang, S.-X. (2007). An accurately delineated Permian-Triassic boundary in continental successions. *Sci. China Ser. D* 50, 1281–1292. doi: 10.1007/s11430-007-0048-2
- Zavialova, N., Blomenkemper, P., Kerp, H., Abu Hamad, A., and Bomfleur, B. (2021). A lyginopterid pollen organ from the upper Permian of the Dead Sea region. *Grana* 60, 81–96. doi: 10.1080/00173134.2020.1772360
- Zeiller, R. (1894). Notes sur la flore des couches permienne de Trienbach (Alsace). *Bull. Soc. Géol. Fr.* 22, 163–182.
- Zeiller, R. (1906). *Bassin Houiller et Permien de Blanzay et du Creusot – Fascicule II: Flore Fossile*. Paris: Études des Gîtes Mineiraux de la France.
- Ziegler, A. M., Hulver, M. L., and Rowley, D. B. (1997). “Permian world topography and climate,” in *Late Glacial and Post-Glacial Environmental Changes – Quaternary, Carboniferous-Permian and Proterozoic*, ed. I. P. Martini (New York, NY: Oxford University Press), 111–146.

Conflict of Interest: The authors declare that the research was conducted in the absence of any commercial or financial relationships that could be construed as a potential conflict of interest.

Copyright © 2021 Blomenkemper, Bäumer, Backer, Abu Hamad, Wang, Kerp and Bomfleur. This is an open-access article distributed under the terms of the Creative Commons Attribution License (CC BY). The use, distribution or reproduction in other forums is permitted, provided the original author(s) and the copyright owner(s) are credited and that the original publication in this journal is cited, in accordance with accepted academic practice. No use, distribution or reproduction is permitted which does not comply with these terms.